Current Applied Physics 11 (2011) e44–e48

Contents lists available at ScienceDirect

Current Applied Physics

journal homepage: www.elsevier.com/locate/cap

Solution-processable fullerene derivatives for organic photovoltaics and n-type thin-film transistors

Sun Young Nam [a], Eun Young Park [a], Tae-Dong Kim [a,*], Shinuk Cho [b], Jea-Gun Park [c], Kwang-Sup Lee [a,*]

[a] Department of Advanced Materials, Hannam University, Daejeon 305-811, Republic of Korea
[b] Department of Physics, University of Ulsan, Ulsan 680-749, Republic of Korea
[c] Department of Electronics and Communications Engineering, Hanyang University, Seoul 133-791, Republic of Korea

ARTICLE INFO

Article history:
Received 4 October 2010
Accepted 29 November 2010
Available online 1 February 2011

Keywords:
Organic photovoltaics
Organic thin-film transistors
Fullerene derivatives
Solution-processing

ABSTRACT

Two solution-processable fullerene derivatives (C_{60}TH-Hx and C_{60}TH-Hx-a) were successfully synthesized for organic photovoltaics and n-type thin-film transistors. The best power conversion efficiency (PCE) was observed in a layered structure of P3HT:C_{60}TH-Hx (PCE = 2.44%), which slightly exceeded that of P3HT:PCBM (PCE = 2.39%). We found a very low PCE for P3HT:C_{60}TH-Hx-a (~0.14%) due to the poor solubility of C_{60}TH-Hx-a. In addition, n-type thin-film transistors were fabricated by solution-processing techniques. The measured values of electron mobility in the devices for PCBM, C_{60}TH-Hx, and C_{60}TH-Hx-a were 5.8×10^{-3}, 2.5×10^{-2}, and 8.5×10^{-4} $cm^2\ V^{-1}\ s^{-1}$, respectively.

1. Introduction

Recently there has been growing interest in organic photovoltaics (OPVs) because of their potential applications in low-cost, flexible, and extremely light-weight solar cells and photodetectors [1–5]. The common OPV configuration is a bulkheterojunction device, in which the active layer consists of a blend of electron-donating materials, for example, poly(3-hexylthiophene) (P3HT), and an electron-accepting material, such as [6,6]-phenyl C61-butyric acid methyl ester (PCBM). The power conversion efficiency (PCE) of the OPVs based on P3HT:PCBM reached over 4% by thermal treatment and solvent annealing under AM 1.5G illumination [6–8]. To further improve the PCE, new conjugated polymer donors and fullerene derivative acceptors are needed for a higher short-circuit current (I_{sc}) and a higher open-circuit voltage (V_{oc}). In recent years, significant efforts have been devoted to develop new low band-gap polymers and PCEs based on these polymers reached 5%–8% [9,10]. However attention has been much less focused on developing new fullerene derivatives in order to surpass or replace the PCBM molecule [11]. Li et al. have investigated the effect of alkyl chain length in the PCBM-like molecules on their photovoltaic properties [12]. Although there was little difference in the absorption spectra and electronic energy level from the molecules, they found that the alkyl chain length exerted a significant influence on the photovoltaic performance. In our recent study, we have reported on a new fullerene derivative (C_{60}TH-Hx) for n-type organic thin-film transistors (OTFTs) [13]. The devices showed an excellent n-channel performance with a highest mobility of 2.8×10^{-2} $cm^2\ V^{-1}\ s^{-1}$. The C_{60}TH-Hx was prepared by a Prato reaction between C_{60} and 3-hexylthiophene-2-carboxaldehyde with *N*-methylglycine, which gives better product yields and purities compared with a synthetic procedure for PCBM. This reaction provides a new pathway to explore molecular engineering of fullerene derivatives with facile synthetic routes.

Herein we designed and synthesized C_{60}TH-Hx-a containing a hexyl group in different positions compared with C_{60}TH-Hx. The photovoltaic performances for C_{60}TH-Hx and C_{60}TH-Hx-a in combination with P3HT were investigated. Furthermore, n-type OTFT devices of the molecules were fabricated by a solution-processing technique and compared with PCBM-based devices.

2. Experimental details

2.1. Chemicals

All reagents were purchased from commercial sources and used without further purification unless otherwise noted. All solvents were purified and freshly distilled prior to use according to

* Corresponding authors. Tel.: +82 42 629 8857; fax: +82 42 629 8854.
E-mail addresses: tdkim@hnu.kr (T.-D. Kim), kslee@hnu.kr (K.-S. Lee).

1567-1739/$ – see front matter © 2011 Elsevier B.V. All rights reserved.
doi:10.1016/j.cap.2010.11.121

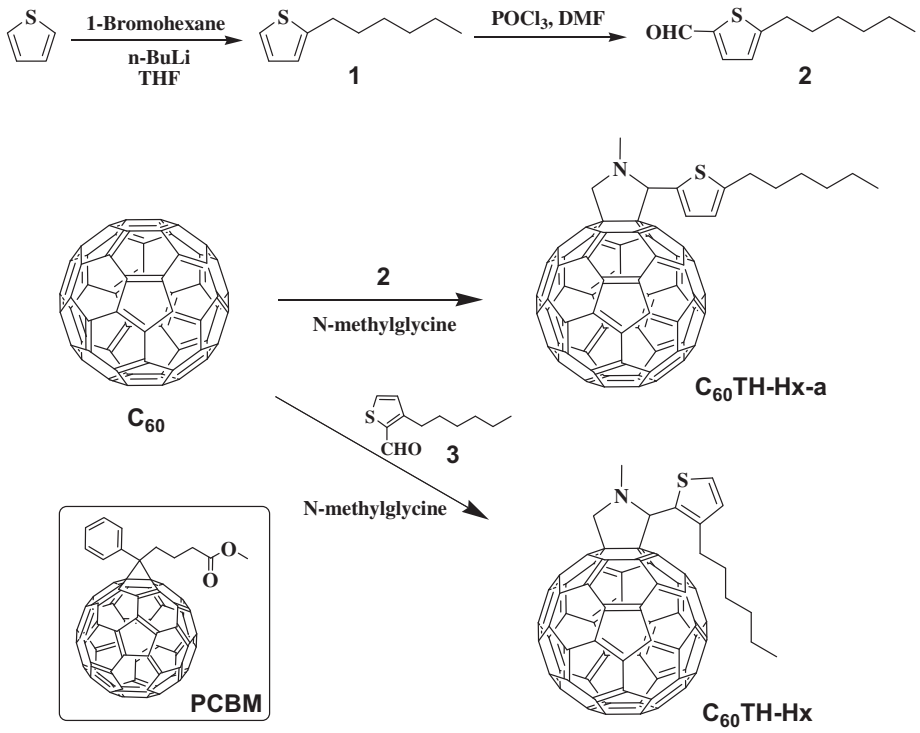

Scheme 1. The molecular structures and synthetic routes for C_{60}TH-Hx and C_{60}TH-Hx-a.

literature procedures. The synthetic procedure of C_{60}TH-Hx was previously reported in the literature [13].

*2.1.1. Synthesis of 2-hexylthiophene (**1**)*

A solution containing thiophene (0.10 mol) in dry THF (120 mL) at −78 °C was treated with 1.6 M of n-BuLi (0.12 mol) in hexane and stirred for 1 h. 1-bromohexane (0.12 mol) in dry THF (20 mL) was slowly added to the solution at −78 °C and the solution was allowed to warm to RT and stirred overnight. The solution was quenched with a saturated NH_4Cl solution and extracted with ether. The combined ether extracts were washed with brine, dried over $MgSO_4$, filtered, and concentrated under a reduced pressure. The resulting crude product was purified by flash chromatography on silica gel with an eluent of hexane to yield compound **1** (yield: 80%). ^{1}H NMR ($CDCl_3$, TMS, ppm): δ 7.07 (d, 1H), 6.86 (t, 1H), 6.73 (d, 1H), 2.81 (t, 2H), 1.69 (m, 2H), 1.30 (m, 6H), 0.83 (t, 3H).

*2.1.2. Synthesis of 5-hexylthiophene-2-carbaldedyde (**2**)*

A solution of DMF (0.10 mol) and dry CH_2Cl_2 (20 mL) at 0 °C, $POCl_3$ (0.10 mol) was slowly added. The mixture was warmed to around 40 °C until a clear pale yellow solution was obtained. The prepared solution was added into a solution of compound **1** (0.08 mol) in dry CH_2Cl_2 (50 mL) at 0 °C. After standing for 12 h at room temperature (RT), aqueous 1 M NaOH was added to the solution for neutralization. Filtration, washing with water, and drying gave light yellow oil. The resulting crude product was purified by flash chromatography on silica gel with an eluent of hexane/CH_2Cl_2 (1:1) to yield compound **2** (yield: 70%). ^{1}H NMR ($CDCl_3$, TMS, ppm): δ 9.74 (s, 1H), 7.53 (d, 1H), 6.83 (d, 1H), 2.80 (m, 2H), 1.64 (m, 2H), 1.26 (m, 6H), 0.82 (t, 3H).

2.1.3. Synthesis of C_{60}TH-Hx-a

A solution of **2** (0.09 mol), fullerene (0.09 mol), and *N*-methylglycine (0.20 mol) in 1,2-dichlorobenzene (30 mL) was refluxed for 48 h. After cooling to RT, the reaction mixture was performed with flash chromatography on silica gel with a gradient eluent of toluene to 20% hexane in toluene. After the crude product was washed and centrifuged with ethanol, recrystallization from 1,4-dioxane yielded the desired product of C_{60}TH-Hx-a (yield: 35%). ^{1}H NMR ($CDCl_3$, TMS, ppm): δ 7.18 (d, 1H), 6.65 (d, 1H), 5.18 (s, 1H), 4.98 (d, 1H), 4.21 (d, 1H), 2.89 (s, 3H), 2.80 (t, 2H), 1.62 (m, 2H), 1.22 (m, 6H), 0.83 (t, 3H). MALDI-TOF-MS (matrix, 2-(4-hydroxyphenylazo)benzoic acid (HABA)): calcd for $C_{67}H_9NS$ 943.14; found 942.28 [M^+]. m.p. 280 °C.

2.2. Characterization

^{1}H NMR spectra (300 MHz) were taken on a Varian 300 spectrometer and mass spectra were recorded on a JMS-AX505WA mass spectrometer. Differential scanning calorimetry (DSC) was performed on a TA instruments Q50 at a ramping rate of 10 °C/min under a nitrogen atmosphere. Atomic force microscopy (AFM) was performed using a Digital Instruments Nanoscope IV operated in tapping mode (~350 kHz frequency, Si tip).

2.3. Photovoltaic device fabrication and measurement

Bulkheterojunction photovoltaic devices were fabricated on an indium tin oxide (ITO) coated glass substrate. Poly(3,4-ethylenedioxylthiophene):poly(styrenesulfonate) (PEDOT:PSS) was spin-coated in air at 5000 rpm for 40 s onto the ITO/glass. The

Table 1
Solubility of PCBM, C_{60}TH-Hx, and C_{60}TH-Hx-a in various solvents.

Materials	Measured solubility (mg/mL)		
	Toluene	Chlorobenzene	Chloroform
PCBM	22	26	13
C_{60}TH-Hx	10	15	<1
C_{60}TH-Hx-a	<1	4	<1

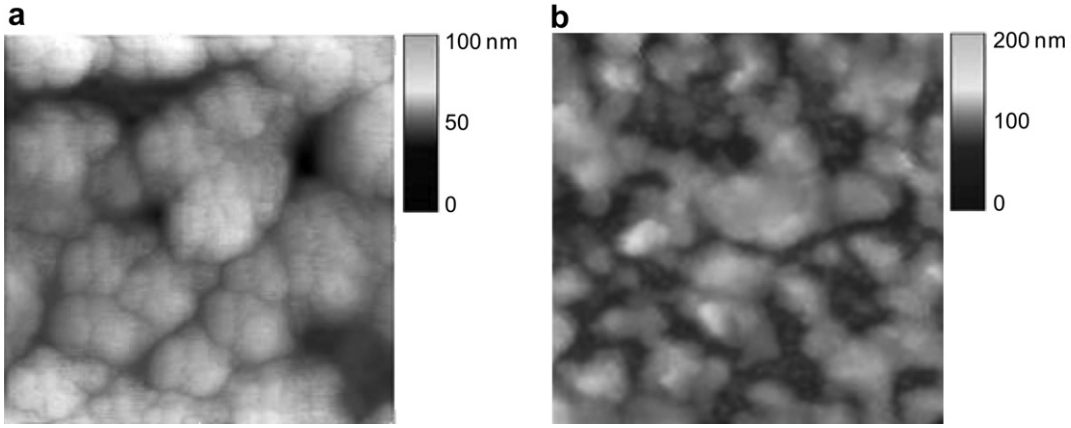

Fig. 1. AFM topographic height images (3 μm × 3 μm) of (a) C_{60}TH-Hx and (b) C_{60}TH-Hx-a films spin-coated on HMDS-treated SiO_2 substrates.

substrate was subsequently dried for 10 min at 140 °C. The blend solutions of P3HT:fullerene derivative (1:1 weight ratio) in 1,2-dichlorobenzene were spin-coated onto the PEDOT:PSS/ITO/glass. TiO_x solution (diluted by 1:200 in methanol) was then spin-coated on top of the film (5000 rpm for 40 s) to perform as a symmetry-breaking and electron extraction layer. The devices were heated at 80 °C for 10 min. Finally, Al metal was deposited by thermal evaporation in a high vacuum (4×10^{-6} mbar). Current–Voltage characteristic curves were measured using a Keithley 2400 source meter. Photovoltaic property was measured using an AM 1.5G illumination (100 mW/cm^2). All devices were encapsulated with UV epoxy and a cover glass (inside a glove box filled with N_2).

2.4. OTFT fabrication and measurement

1.0 wt% of active organic semiconductors in 1,2-dichlorobenzene were spin-coated onto the SiO_2 substrates treated with hexamethyldisilazane (HMDS). A film thickness of 30–50 nm was obtained at a spin rate of 2000 rpm for 60 s. Bilayer top-contact electrodes consisting of Mg/Al (10 nm/120 nm) were evaporated under high vacuum (10^{-6} mbar) through a shadow mask. All the OTFT devices were encapsulated by a glass can and getters in an inert argon environment inside a glove box system. Electrical measurements were performed at RT under an argon atmosphere using an HP4156C semiconductor parameter analyzer.

3. Results and discussion

The synthetic approach for C_{60}TH-Hx and C_{60}TH-Hx-a is depicted in Scheme 1. The hexyl group was introduced to the 2- and 3-position in thiophene to afford 2-hexylthiophene and 3-hexylthiophene, respectively. 5-hexylthiophene-2-carbaldedyde (compound **2**) and 3-hexylthiophene-2-carbaldedyde (compound **3**) were synthesized by the Vilsmeier reaction. C_{60}TH-Hx-a (or C_{60}TH-Hx) was obtained by the Prato reaction between fullerene and compound **2** (or **3**) with N-methylglycine refluxing in 1,2-dichlorobenzene for 48 h. The thermal property of C_{60}TH-Hx-a and C_{60}TH-Hx was evaluated by differential scanning calorimetry (DSC) in a nitrogen atmosphere at a rate of heating of 10 °C/min. Upon heating, one endothermic peak at 280 °C and 220 °C corresponding to the crystalline-to-isotropic phase transition was observed for C_{60}TH-Hx-a and C_{60}TH-Hx, respectively.

Table 1 shows quantitative solubility of C_{60}TH-Hx-a, C_{60}TH-Hx, and PCBM in various solvents at 25 °C. C_{60}TH-Hx and PCBM were readily soluble in aromatic solvents, such as chlorobenzene, while C_{60}TH-Hx-a dissolved poorly in such solvents. C_{60}TH-Hx-a has an alkyl chain on the thiophene with a different position compared to C_{60}TH-Hx. The alkyl chain of C_{60}TH-Hx-a can extend outwards from the fullerene unit resulting in high crystallinity and poor solubility.

Structural characterization of spin-coated C_{60}TH-Hx-a and C_{60}TH-Hx on HMDS-treated SiO_2/Si substrates was performed by AFM. Fig. 1 shows topography images (3 × 3 μm) of both films.

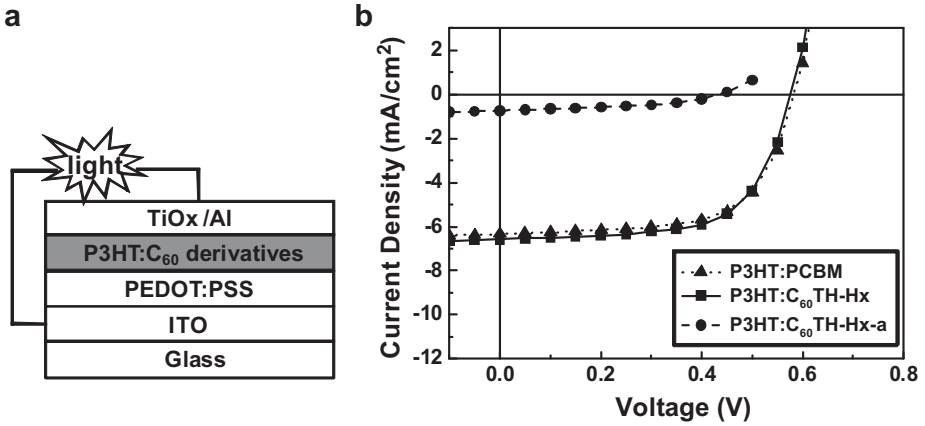

Fig. 2. (a) A schematic of OPV device architecture and (b) current–voltage (I–V) characteristics of OPV devices for P3HT:PCBM (triangle), P3HT:C_{60}TH-Hx (square), and P3HT:C_{60}TH-Hx-a (circle) under AM 1.5G illumination.

Table 2
Photovoltaic performance of the devices based on the blend of P3HT with PCBM, C_{60}TH-Hx, and C_{60}TH-Hx-a (1:1 w/w) under AM 1.5G illumination.

Materials	I_{sc} (mA/cm^2)	V_{oc} (V)	FF	PCE (%)
P3HT:PCBM	6.32	0.58	0.65	2.39
P3HT:C_{60}TH-Hx	6.58	0.58	0.64	2.44
P3HT:C_{60}TH-Hx-a	0.73	0.43	0.44	0.14

Densely packed grains with average diameters of about 200–600 nm were observed throughout the image in the C_{60}TH-Hx film. The more irregular grain sizes and less uniform surface were exhibited in C_{60}TH-Hx-a, indicating a pronounced tendency of crystallite aggregation for C_{60}TH-Hx-a. The microstructures of C_{60}TH-Hx-a and C_{60}TH-Hx will be further investigated by X-ray diffraction (XRD) measurements.

Bulkheterojunction photovoltaic devices with a 100 nm thick composite film (weight ratio of P3HT:fullerene derivatives = 1:1) as the active layer were fabricated by spin-coating from chlorobenzene solution on the top of a pre-patterned ITO substrate covered by 100 nm of PEDOT:PSS. In the case of the device with a TiO_x layer, the TiO_x precursor solution was applied in air on the top of the P3HT:fullerene derivative composition. It serves as an optical spacer to increase the PCE by creating more photogenerated charge carriers in the bulkheterojunction layer [14]. Subsequently a thin layer of aluminum was thermally deposited under a vacuum (Fig. 2(a)).

The photovoltaic characteristics were measured under an AM 1.5G solar simulator. The power conversion efficiency, PCE, and fill factor, FF, were calculated by the following equations:

$$\mathrm{PCE} = \mathrm{FF} \times I_{sc} \times V_{oc}/P_{in} \quad (1)$$

$$\mathrm{FF} = I_m V_m / I_{sc} V_{oc} \quad (2)$$

where P_{in} is the incident radiation flux, I_{sc} and V_{oc} are the short-circuit current density and open-circuit voltage, respectively, and I_m and V_m are the current and voltage for maximum power output, respectively. The optimized device performances are summarized in Table 2. The current–voltage curves of the devices based on the three blending systems, P3HT:PCBM, P3HT:C_{60}TH-Hx, and P3HT:C_{60}TH-Hx-a, are shown in Fig. 2(b). The P3HT:PCBM device serves as a reference for the comparison of the efficiencies of the newly synthesized fullerene derivatives. The best performance is observed in the P3HT:C_{60}TH-Hx, which exhibits the PCE of 2.44% with I_{sc} = 6.58 mA/cm^2, V_{oc} = 0.43 V, and FF = 0.64. These values are slightly higher than those of the P3HT:PCBM device (PCE = 2.39%). Since the electronic states of the C_{60} portions in C_{60}TH-Hx and PCBM are expected to be similar due to the linkers added to a 6:6 ring juncture of C_{60} [15], they hardly influenced the photovoltaic properties for both devices. However, in the case of P3HT:C_{60}TH-Hx-a, the PCE significantly decreased to 0.14%. As mentioned earlier, C_{60}TH-Hx-a has poorer solubility than C_{60}TH-Hx due to the alkyl chain extended outwards from the fullerene unit, which resulted in irregular grain sizes and inhomogeneous surface in the film. Therefore, the poorer PCE of the P3HT:C_{60}TH-Hx-a device may be due to the morphology and interface of the films. Similar behavior appeared on the OTFT performance for PCBM, C_{60}TH-Hx, and C_{60}TH-Hx-a.

To explore the electron transport properties of PCBM, C_{60}TH-Hx, and C_{60}TH-Hx-a, n-type transistors were fabricated on HMDS-treated SiO_2 substrates by spin-coating from 1,2-dichlorobenzene solution under ambient conditions. Mg/Al source and drain electrodes were deposited on the films by using thermal evaporation under a high vacuum. The channel length (L) and width (W) of the transistors were 50 μm and 3 mm, respectively. The OTFT device geometry is shown in Fig. 3(a). The electron transfer characteristics were compared in Fig. 3(b)–(d) for PCBM with a drain voltage (V_D)

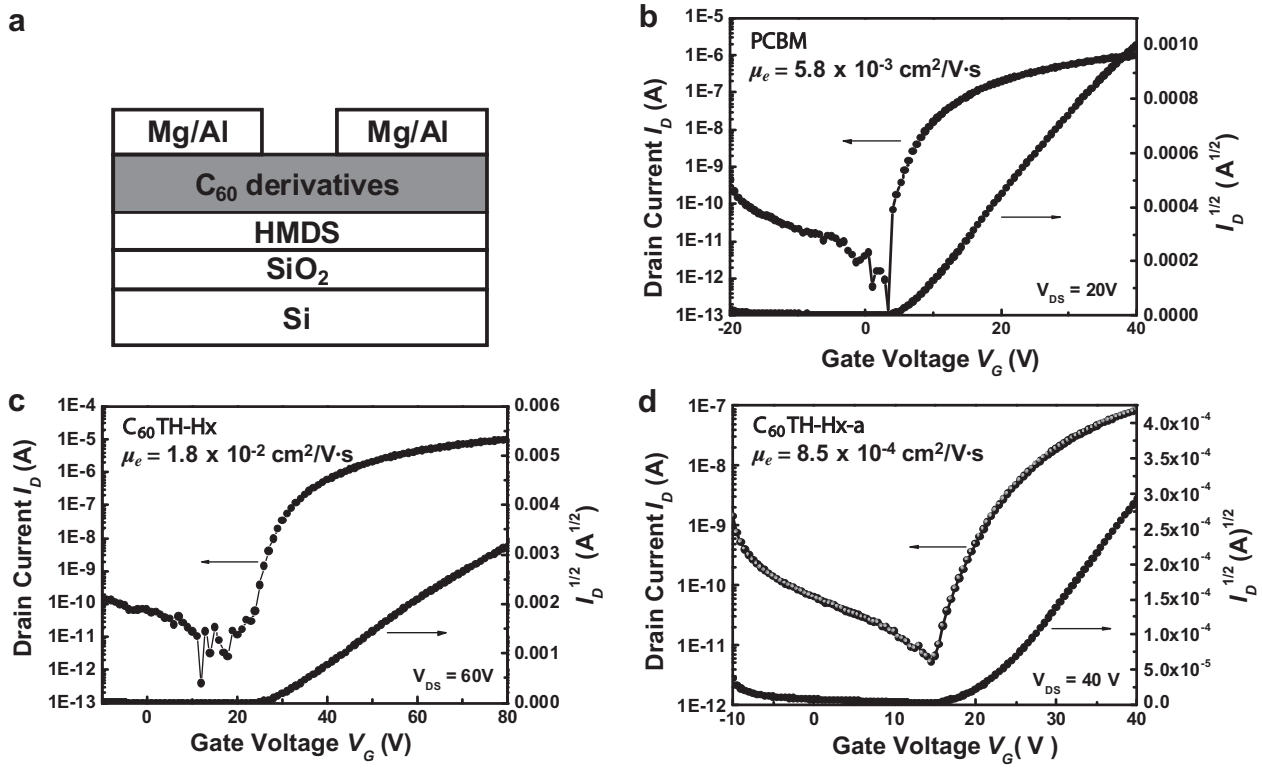

Fig. 3. (a) A schematic of OTFT device architecture and transfer characteristics of the drain current versus gate voltage (I_D–V_G) and the square root of drain current–gate voltage ($I_D^{1/2}$–V_G) for (b) PCBM, (c) C_{60}TH-Hx, and (d) C_{60}TH-Hx-a device.

Table 3
OTFT performance of spin-coated PCBM, C_{60}TH-Hx, and C_{60}TH-Hx-a devices on HMDS-treated SiO_2 substrates.

Materials	Spin speed (rpm)	Mobility (cm^2/V s)	I_{on}/I_{off} ratio	Threshold volt (V)
PCBM	2000	5.8×10^{-3}	$\sim 1 \times 10^4$	18
C_{60}TH-Hx	2000	1.8×10^{-2}	$\sim 1 \times 10^5$	14
C_{60}TH-Hx-a	1000	8.5×10^{-4}	$\sim 1 \times 10^5$	21

of 20 V, C_{60}TH-Hx with a V_D of 60 V, and C_{60}TH-Hx-a with a V_D of 40 V, respectively. All devices exhibited excellent n-type transistor characteristics. The electron mobility (μ_e) and the threshold voltage (V_T) were estimated from the square root of drain current − gate voltage ($I_D^{1/2} - V_G$) plots, according to the standard equation in the saturation regime, $I_D = (W/2L)\mu_e C_i(V_G - V_T)$, where I_D is the drain current, W and L are the conduction channel width and length, respectively, C_i is the capacitance per unit area of gate dielectric, and V_G is the gate voltage. The electron mobilities were in the range of $\mu_e = 5.8 \times 10^{-3}$ cm^2/V s for PCBM, 1.8×10^{-2} cm^2/V s for C_{60}TH-Hx, and 8.5×10^{-4} cm^2/V s for C_{60}TH-Hx-a. In Table 3, OTFT properties of each device are summarized. Among the OTFT devices, the lowest mobility value was observed in the C_{60}TH-Hx-a, which exhibited the poorest photovoltaic performance. The C_{60}TH-Hx device exhibited the best performance with a highest mobility of 1.8×10^{-2} cm^2/V s with the on/off current ratio (I_{On}/I_{Off}) of $\sim 1.0 \times 10^5$ and a V_T of 14 V. Interestingly, we could utilize an ink-jet-printing method for C_{60}TH-Hx in order to fabricate OTFT devices exhibiting higher mobility (2.8×10^{-2} cm^2/V s) and a lower V_T (7 V) than the spin-coated device [13]. This indicates that suitable modification of the fullerene can provide an opportunity to find alternatives of PCBM without deterioration of its photovoltaic and OTFT performances.

4. Conclusion

We have synthesized fullerene derivatives, C_{60}TH-Hx and C_{60}TH-Hx-a, and compared with PCBM with regards to the characterization of photovoltaics and OTFTs. The thin-film devices were fabricated by solution-processable techniques, such as spin-coating. The C_{60}TH-Hx blended with P3HT (1:1) exhibited best photovoltaic performance (PCE = 2.44%) compared with PCBM and C_{60}TH-Hx-a. In addition, the C_{60}TH-Hx showed excellent OTFT characteristics, which possessed a highest mobility of 1.8×10^{-2} cm^2/V s with an I_{On}/I_{Off} of $\sim 1.0 \times 10^5$ and a V_T of 14 V.

Acknowledgements

This study was supported by the National Research Program for Terabit Nonvolatile Memory Development and the Fundamental R&D Program for Core Technology of Materials (M2007010004) funded by the Ministry of Knowledge Economy and also by the Mid-career Researcher Program through NRF grant funded by the MEST (No. 2010-0000499). T.-D. Kim acknowledges supports from Korea National Research Foundation (NRF-2009-0076833).

References

[1] G. Yu, J. Gao, J.C. Hummelen, F. Wudl, A.J. Heeger, Science 270 (1995) 1789.
[2] S. Gunes, H. Neugebauer, N.S. Sariciftci, Chem. Rev. 107 (2007) 1324.
[3] B.C. Thompson, J.M.J. Frechet, Angew. Chem. Int. Ed. 47 (2008) 58.
[4] Y.-J. Chen, S.-H. Yang, C.-S. Hsu, Chem. Rev. 109 (2009) 5868.
[5] J.W. Chen, Y. Cao, Acc. Chem. Res. 42 (2009) 1709.
[6] W.L. Ma, C.Y. Yang, X. Gong, K.H. Lee, A.J. Heeger, Adv. Funct. Mater. 15 (2005) 1617.
[7] G. Li, V. Shrotriya, J.S. Huang, Y. Yao, T. Moriarty, K. Emery, Y. Yang, Nat. Mater. 4 (2005) 864.
[8] Y. Zhao, Z.Y. Xie, Y. Qu, Y.H. Geng, L.X. Wang, Appl. Phys. Lett. 90 (2007) 043504.
[9] H.-Y. Chen, J.H. Hou, S.Q. Zhang, Y.Y. Liang, G.W. Yang, Y. Yang, L.P. Yu, Y. Wu, G. Li, Nat. Photon. 3 (2009) 649.
[10] S.H. Park, A. Roy, S. Beaupré, S. Cho, N. Coates, J.S. Moon, D. Moses, M. Leclerc, K.H. Lee, A.J. Heeger, Nat. Photon. 3 (2009) 297.
[11] C. Yang, J.Y. Kim, S. Cho, J.K. Lee, A.J. Heeger, F. Wudl, J. Am. Chem. Soc. 130 (2008) 6444.
[12] G. Zhao, Y. He, Z. Xu, J. Hou, M. Zhang, J. Min, H.-Y. Chen, M. Ye, Z. Hong, Y. Yang, Y. Li, Adv. Funct. Mater. 20 (2010) 1480.
[13] E.Y. Park, J.S. Park, T.-D. Kim, K.-S. Lee, H.S. Lim, J.S. Lim, C. Lee, Org. Electron. 10 (2009) 1028.
[14] J.Y. Kim, S.H. Kim, H.-H. Lee, K. Lee, W. Ma, X. Gong, A.J. Heeger, Adv. Mater. 18 (2006) 572.
[15] M. Chikamatsu, S. Nagamatsu, Y. Yoshida, K. Saito, K. Yase, Appl. Phys. Lett. 87 (2005) 203504.